

See discussions, stats, and author profiles for this publication at: <https://www.researchgate.net/publication/227880861>

Laser photolysis studies of hydrazine vapor: 193 and 222-nm H-atom primary quantum yields at 296 K, and the kinetics of H + N₂H₄ reaction over the temperature range 222–657 K

ARTICLE in INTERNATIONAL JOURNAL OF CHEMICAL KINETICS · AUGUST 1995

Impact Factor: 1.52 · DOI: 10.1002/kin.550270805

CITATIONS

21

READS

20

1 AUTHOR:



Ghanshyam Vaghjiani

United States Air Force

60 PUBLICATIONS 1,471 CITATIONS

SEE PROFILE

Laser Photolysis Studies of Hydrazine Vapor: 193 and 222-nm H-atom Primary Quantum Yields at 296 K, and the Kinetics of $\text{H} + \text{N}_2\text{H}_4$ Reaction over the Temperature Range 222–657 K

GHANSHYAM L. VAGHJIANI

*Hughes STX, Phillips Laboratory, PL/RKFA,
10 E. Saturn Blvd, Edwards Air Force Base, California 93524*

Abstract

The primary quantum yield of H-atom production in the pulsed-laser photolysis of hydrazine vapor, $\text{N}_2\text{H}_4 + h\nu \rightarrow \text{H} + \text{N}_2\text{H}_3$, was measured to be (1.01 ± 0.12) at 193 nm relative to HBr photolysis, and (1.06 ± 0.16) at 222 nm relative to 248-nm N_2H_4 photolysis, in excess He buffer gas at 296 K. The H-atoms were directly monitored in the photolysis by cw-resonance fluorescence detection of $\text{H}(^2\text{S})$ at 121.6 nm. The high H-atom yield observed in the photolysis is consistent with the continuous ultraviolet absorption spectrum of N_2H_4 involving unit dissociation of the diamine from repulsive excited singlet state(s). The laser photodissociation of N_2H_4 was thus used as a 'clean' source of H-atoms in excess N_2H_4 and He buffer gas to study the gas-phase reaction, $\text{H} + \text{N}_2\text{H}_4 \rightarrow \text{products}$; (k_1), in a thermostated photolysis reactor made of quartz or Pyrex. The pseudo-first-order temporal profiles of $[\text{H}]$ decay immediately after photolysis were determined for a range of different hydrazine concentrations employed in the experiments to calculate the absolute second-order reaction rate coefficient, k_1 . The Arrhenius expression was determined to be $k_1 = (11.7 \pm 0.7) \times 10^{-12} \exp[-(1260 \pm 20)/T] \text{ cm}^3 \text{ molec}^{-1} \text{ s}^{-1}$ in the temperature range 222–657 K. The rate coefficient at room temperature was, within experimental errors, independent of the He buffer gas pressure in the range 24.5–603 torr. The above temperature dependence of k_1 is in excellent agreement to that we determine in our discharge flow-tube apparatus in the temperature range 372–252 K and in 9.5 torr of He pressure. The Arrhenius parameters we report are consistent with a metathesis reaction mechanism involving the abstraction of hydrogen from N_2H_4 by the H-atom. © 1995 John Wiley & Sons, Inc.

Introduction

The reaction of atomic hydrogen with hydrazine (N_2H_4) is of interest because of its importance in several chemical systems. The reaction is involved during photochemical decomposition of N_2H_4 as in laboratory photolysis [1] and in Jupiter's lower atmosphere [2], and as one of the chain propagation steps in pyrolytic decomposition of N_2H_4 [3]. There have been five previous gas-phase rate coefficient determinations for this reaction that cover a combined temperature range of 228–536 K. However, there exist serious discrepancies among the reported Arrhenius temperature dependences of the rate coefficient for this reaction. In the discharge flow reactor kinetics investigations of Gehring et al. [4], Schiavello and Volpi [5], and Chobanyan et al. [6] similar values for the activation energy in the range from about 2.0 to 2.5 kcal mol⁻¹ were measured, but Francis and Jones [7] reported a lower value of ca. 1.3 kcal mol⁻¹. In these experiments, the value of the preexponential factor differs considerably, ranging from about 5.8×10^{-13} to $6.8 \times 10^{-12} \text{ cm}^3 \text{ molec}^{-1} \text{ s}^{-1}$. Stief and Payne [8] carried out their investigations in a flash-photolysis reactor and reported an activation energy of

ca. 2.4 kcal mol⁻¹ and a preexponential factor of ca. 9.9×10^{-12} cm³ molec⁻¹ s⁻¹, in reasonable agreement with only the study of Chobanyan and co-workers [6].

We have undertaken this gas-phase kinetics study of H-atoms with hydrazine in an attempt to establish the correct Arrhenius activation energy and preexponential factor which are required for the proper modeling of the above decomposition processes. In this work the pseudo-first-order temporal profile of H-atom concentration decay in a known excess of hydrazine concentration in He buffer was determined by time-resolved resonance fluorescence detection of H(²S) at 121.6 nm immediately after optically thin laser photolysis of N₂H₄ at 248 nm. Since the atomic species decays exponentially, we need only determine its relative concentration precisely as a function of time which is very accurately known in our experiments. We accurately determine the [N₂H₄] by near-ultraviolet photometry and by measuring the cell pressure and the mass rates of He carrier buffer gas and N₂H₄ flows that provide the desired levels of the reactant concentrations in the reaction zone. We are thus able to determine the N₂H₄ concentrations, and hence k_1 to within ca. $\pm 15\%$. Also, we avoid interference from secondary reactions in our rate coefficient measurements by employing large ratios of hydrazine to initial H-atom concentration. Such interference and ill-defined reagent concentrations may have led to the erroneous values reported in previous studies. Furthermore, we have also repeated the rate coefficient measurements for this reaction in our newly constructed discharge flow-tube apparatus [9]. The results from this experiment compare extremely well with our photolysis work and provide support for the lack of any significant systematic errors in the rate coefficients we report here.

Recently [1] we reported the room temperature ultraviolet absorption spectrum of gaseous hydrazine where we also reviewed earlier photochemical studies on this molecule. We directly measured the primary quantum yield for H-atom production at 248 nm to be (0.85 ± 0.15) relative to CH₃SH photolysis which undergoes unit dissociation via S—H bond cleavage [10]. This result was in agreement with the indirect quantum yield of (0.97 ± 0.10) deduced by Schurath and Schindler [11] at 206.2 nm from the measured H₂ end-product yields in their experiments. Thus it appears that absorption of light in this long wavelength tail due to the weak electronic transition to the first excited singlet \tilde{A}^1A state results in unit dissociation of the molecule via cleavage of the stronger [12] N—H bond. At wavelength, λ , <206 nm the N₂H₄ spectrum shows a shoulder due to the onset of a transition to the next excited singlet \tilde{B}^1B state with stronger diffuse bands in the vacuum-uv for excitation to even higher states [13–16]. Previous photolysis work of Lindberg et al. [17] at 193 nm, and that of Biehl and Stuhl [14] and Vinogradov and Firsov [18] in the vacuum-uv showed that the absorption of a single uv-photon was accompanied by visible emission from the excited amidogen radical (NH₂(A)) formed in the direct dissociation channel, $N_2H_4 + h\nu \rightarrow NH_2(\tilde{A}^2A_1) + NH_2(\tilde{X}^2B_1)$. The room temperature threshold for this reaction is at ca. 293 nm [19]. The absolute quantum yield for the reaction in which the weaker [12] N—N bond is cleaved was not reported, though it was concluded that the quantum yield for the visible emission was small of the order of a few percent at the most. Other studies have also reported formation of the excited state imidogen radical (NH(A)) in hydrazine photolysis [14,17,20]. This can be explained to be due to secondary photolysis of the primary photofragments and not as a result of direct N₂H₄ dissociation. Ramsay [21], and Husain and Norrish [22] recorded transient absorption spectra of the amidogen radical (NH₂) upon flash-photolysis of N₂H₄ as did Arvis and co-workers [23]. The latter authors concluded that the bulk of the NH₂ radical was

being formed in subsequent secondary reactions after the initial flash and not in the primary photolysis of N_2H_4 which Ramsay, and Husain and Norrish had incorrectly assumed to occur via the splitting of the N—N bond in hydrazine. Also, primary $\text{ND}_2(\text{A})$ visible emission and secondary $\text{ND}(\text{A})$ ultraviolet emission has been observed [17] in 193-nm excitation of N_2D_4 which exhibits an absorption spectrum similar to that of N_2H_4 [15].

To further extend and quantify the direct H-atom product yield measurements in hydrazine photolysis, we report here the laser photodissociation of N_2H_4 at 193 and 222 nm. To avoid an absolute measurement of the yield of H-atoms in N_2H_4 photolysis we use a relative technique in which a reference back-to-back experiment is performed under similar photolytic conditions where the quantum yield of H-atoms has previously been established. The initial $\text{H}(^2\text{S})$ resonance fluorescence signal in this latter experiment is used to normalize that measured in the former to accurately calculate the H-atom primary quantum yields at 193 and 222 nm. Our results show that, despite the numerous dissociation channels energetically accessible at the photolyzing wavelengths [1], the major primary process is the cleavage of the N—H bond, with a quantum yield close to unity for H-atom production.

Experimental Technique

We have described in detail the operation of our photolysis apparatus elsewhere [1,10,24]. Therefore, here we only give those experimental procedures to understand the methodology used in measuring the gas-phase reaction rate coefficient, k_1 , for the reaction $\text{H} + \text{N}_2\text{H}_4$, and for determining the H-atom primary quantum yields in N_2H_4 photolysis. A small sample of liquid hydrazine is vaporized and carried into an absorption cell for 213.9 or 253.7-nm photometric determination of the gas-phase concentration in the He flow. The N_2H_4 uv-absorption cross sections [1] of $\sigma_{213.9} = 220 \times 10^{-20}$ and $\sigma_{253.7} = 2.86 \times 10^{-20} \text{ cm}^2 \text{ molec}^{-1}$ were used to calculate the concentration using the Beer-Lambert law. This flow is further diluted in a flow of He before sending it to the photolysis reactor under 'slow-flow' conditions with linear velocity of the gas in the range $1.5\text{--}33 \text{ cm s}^{-1}$ across the reaction zone. The number density of N_2H_4 in the reaction zone is calculated from the known flow rates used to carryout the dilution, and the measured cell pressure and temperature at the reaction zone. The electronic mass flow meters, the capacitance manometers and the chromel-alumel thermocouples used had previously been calibrated. $[\text{N}_2\text{H}_4]$ was typically in the range $(2\text{--}200) \times 10^{14} \text{ molec cm}^{-3}$. The N_2H_4 is photolyzed under optically thin conditions using a 20-ns pulsed 248-nm excimer laser beam (operating at 2 to 10 Hz). The initial H-atom concentration, $[\text{H}]_0$, is kept low, typically 1×10^{10} to $1 \times 10^{12} \text{ molec cm}^{-3}$, and is estimated in our experiments from the known laser beam area and fluence, the photodissociation quantum yield of H, the absorption cross section at the photolysis wavelength, and the measured $[\text{N}_2\text{H}_4]$ in the reactor. As the photolysis is carried out in excess He buffer gas the intrinsic translationally hot hydrogen atoms (H^*) produced in the photolysis are instantly thermalized [25] by collisions with the excess buffer gas before a significant amount of reaction occurs with N_2H_4 . The excess He gas pressure was in the range 24.5–603 torr. Thus in our experiments we should observe an instantaneous rise in the H-atom signal, synchronous with the laser pulse (due to initial photolytic production and thermalization) followed by an exponential decay due to mainly reaction of thermalized H with N_2H_4 , and to a small extent, due to its diffusion out of

the detection zone. The pseudo-first-order temporal profile of H-atoms in our reactor is monitored by cw-resonance fluorescence. A lamp consisting of an electrodeless microwave discharge through a few torr of He is used to excite ($1s, {}^2S_{1/2} \rightarrow 2s, {}^2P_{1/2,3/2}$) transition in H-atoms at 121.6 nm. The output of the lamp is coupled to the reactor orthogonally to the photolysis beam using a MgF_2 lens and the region between the lamp and the reactor purged with O_2 (1200 torr cm) to filter out O-atom and N-atom emission lines from the discharge lamp. The resonance fluorescence ensuing from the reaction zone is collected along the third orthogonal axis using a MgF_2 lens and imaged through another O_2 cell and onto the photocathode of a solar-blind photomultiplier tube (PMT). The extraneous long-lived reactor fluorescence that is excited by the laser-flash was minimized by use of appropriate light-baffles that reduced laser scattering within the cell. The output of the PMT is fed via a photon counting device to a multichannel scaler. The temporal profile of [H] is followed by recording the fluorescence signal in 30 (or 50 or 100) μs dwell time intervals until it decays down to the background level observed prior to photolysis. The background level is determined by pretriggering the multichannel scaler 10 ms before the arrival of the photolysis laser pulse. The background corrected fluorescence signal is known to be directly proportional to the [H] in the reactor. Up to 5000 temporal profiles are co-added to obtain a well defined [H] decay (typically over 3 lifetimes). The data is stored in a microcomputer for later analysis.

At a given temperature, which ranged from 222 to 657 K, [H] temporal profiles were recorded for a range of N_2H_4 concentrations employed in the experiments. For kinetic studies below room temperature, a double-wall-250-cc Pyrex reactor was used. Cool thermostated ethanol was flowed between the jacket of the outer and inner walls of the reactor to obtain the desired reaction temperature. The gas temperature inside the cell was stable to within ± 1 K as measured by the thermocouple situated just above the reaction zone. The lowest temperature used was 222 K below which it became difficult to accurately measure the rate coefficient because of the rapidly falling hydrazine saturated vapor pressure and the slowing down of the reaction rate. Kinetic studies at above room temperature were carried out in a similarly sized quartz reaction cell that was resistively heated. Although we could heat this cell to ca. 1000 K or so, it was found that the hydrazine was undergoing significant heterogeneous decomposition at temperatures greater than ca. 657 K. This was inferred from the photometric measurements of the N_2H_4 in the gas mixture exiting our quartz cell.

The H-atom yield in 222-nm photolysis of N_2H_4 was measured at 296 K relative to photolysis at 248 nm in a back-to-back experiment, keeping $[N_2H_4]$ constant. The 222 and 248 laser beams were carefully collimated and made to illuminate the same reaction volume in the reactor. The excimer laser outputs were known to be stable to within ca. $\pm 5\%$, and the fluence of the beams was determined at the exit window of the reactor using a calibrated calorimeter. The H-atom yield in 193-nm photolysis of N_2H_4 was measured relative to 193-nm photolysis of hydrogen bromide in back-to-back experiments at a constant laser fluence. The hydrogen bromide was introduced into the reactor by replacing the N_2H_4/He flow with a HBr/He flow from a standard 1% stock mixture contained in a 12- ℓ Pyrex bulb followed by further dilution in He to obtain the desired [HBr] in the reaction zone. The microwave lamp is known to be stable during the course of these back-to-back experiments. The detection sensitivity of our apparatus for H has been determined to be typically ca. 1×10^8 molec cm^{-3} for a signal-to-noise ratio of 1 and one second integration time.

Ultra pure hydrazine (98.4%) was supplied by Edwards AFB. The hydrazine is known to be free of hydrocarbon and NH_3 impurities. The balance of water (1.6%) is reduced in our samples by repeated evaporation, and is not expected to cause any interference in our experiments. HBr (99.8%) supplied by Matheson Gas Products was purified by several freeze-thaw cycles at a grease-less vacuum line, and standard 1% stock mixtures made up in He and stored in darken 12- ℓ Pyrex bulbs. H_2 (99.999%) from Linde was used as supplied to make 1% mixtures in He for the discharge gas in the flow-tube experiments. He (99.9997%) from U.S. Bureau of Mines and O_2 (99.991%) from Big Three Industries were used as received.

Results

Rate Coefficient Measurements

Since the $[\text{N}_2\text{H}_4]$ is always in a great excess over the $[\text{H}]$ produced in the photolysis, it can be shown that the temporal profile of H-atoms immediately after photolysis is given by $[\text{H}]_t = [\text{H}]_0 e^{-k't}$, where $[\text{H}]_t$ and $[\text{H}]_0$ are the H-atom concentrations at time t and zero, respectively. The constant, k' , is given by $k' = k_1[\text{N}_2\text{H}_4] + k_d$ and represents the pseudo-first-order rate coefficient for $[\text{H}]$ decay in the photolysis reactor. k_d is the sum of the first-order rate coefficients due to mainly, diffusion of H out of the detection zone, and to, a small extent, reaction of H with background impurities. It is measured in the absence of hydrazine in the photolysis of dilute O_3/H_2 mixtures in He, and is found to be small, typically of the order of ca. 30 s^{-1} . k_1 is the second-order rate coefficient for reaction of H with N_2H_4 . Figure 1 shows

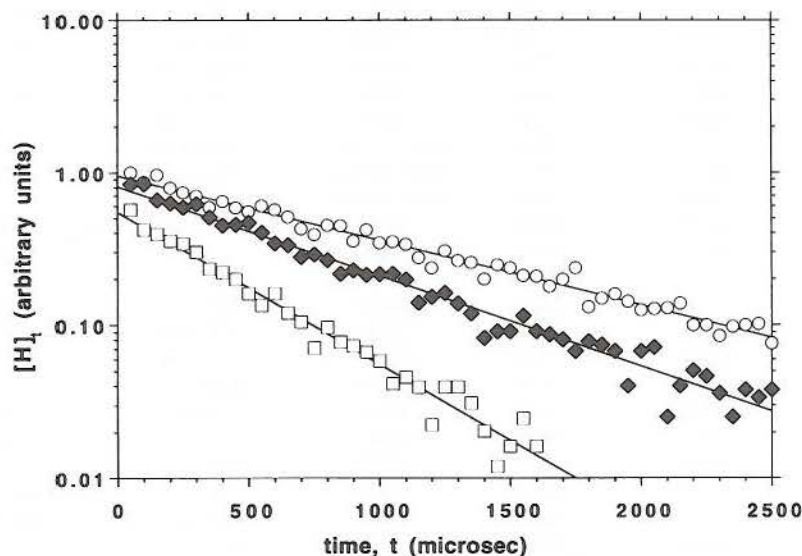


Figure 1. Typical $[\text{H}]_t$ temporal profiles immediately after 248-nm photolysis of N_2H_4 at 296 K. Each data point is the background corrected H-atom fluorescence signal collected in 50- μs dwell-time bins that has been co-added for 2000 photolytic pulses. $[\text{N}_2\text{H}_4] = 5.29 \times 10^{15}$ (open circles), 7.82×10^{15} (closed diamonds), and $15.29 \times 10^{15} \text{ molec cm}^{-3}$ (open squares). Solid lines are fit to data points whose slopes yield a value for the pseudo-first-order rate coefficient, k' , for $[\text{H}]$ decay in the reactor, and the intercepts give a measure of the initial H-atom primary yields in the photolyses.

typical [H] temporal profiles obtained for three different N_2H_4 concentrations. The data shows an instantaneous rise in the H-atom signal upon photolysis of N_2H_4 and well-behaved exponential decays of [H]. The lines represent exponential fit to the data points. The slope of the line gives a value for the pseudo-first-order decay rate coefficient, k' . k' values typically ranged from about 50 to 6750 s^{-1} . The absolute second-order rate coefficient, k_1 , was calculated from the slope of a plot of k' vs. $[\text{N}_2\text{H}_4]$. Each k_1 calculation typically involved k' measurements at five to ten different N_2H_4 concentrations. Our k_1 values are given in Table I and shown as a function of $1/T$ in Figure 2 together with previous data.

TABLE I. Absolute second-order reaction rate coefficients, k_1 , for the gas-phase reaction $\text{H} + \text{N}_2\text{H}_4 \rightarrow$ products, and the experimental parameters used.

Temperature T (K)	He buffer gas pressure (torr)	Linear flow gas velocity (cm s^{-1})	$[\text{N}_2\text{H}_4]/[\text{H}]_0$ range ^a	$[\text{N}_2\text{H}_4]$ range (1×10^{15} molec cm^{-3})	k_1 (1×10^{-13} $\text{cm}^3 \text{ molec}^{-1} \text{ s}^{-1}$) ^d
222	182.0	4.7	4000	0.2–1.4	0.424 ± 0.038
222	186.0	4.9	11500	0.5–1.6	0.402 ± 0.069
230	41.0	17.8	13500	0.7–2.6	0.488 ± 0.065
232	103.0	8.7	32000	0.6–3.0	0.589 ± 0.082
232	110.0	9.2	8000	0.5–3.2	0.507 ± 0.052
233	106.0	9.3	32000	0.5–3.0	0.600 ± 0.073
250	40.0	6.0	16000	1.0–13.4	0.764 ± 0.026
250	39.0	6.1	16000 ^b	0.9–16.7	0.723 ± 0.063
273	41.0	6.2	16000	0.8–10.5	1.05 ± 0.07
273	42.0	7.0	11500	1.2–16.5	1.10 ± 0.08
290	603	1.5	5000	0.5–3.9	1.33 ± 0.05
293	31.8	7.0	1500 ^c	0.2–1.0	1.38 ± 0.10
293	162.0	5.8	5000	0.6–2.4	1.40 ± 0.03
294	160.0	5.9	1500	0.7–3.5	1.52 ± 0.04
296	24.5	7.4	4000	0.4–3.6	1.44 ± 0.04
296	37.0	5.0	4500–11500	2.9–10.8	1.47 ± 0.11
321	40.0	8.0	6000–20000	1.0–12.2	2.19 ± 0.11
371	41.0	9.0	6000–8000	1.7–11.2	3.85 ± 0.28
400	42.0	10.0	5500	1.0–8.2	5.12 ± 0.26
420	40.0	10.0	5000–8000 ^b	1.5–8.4	7.08 ± 0.40
420	40.0	10.0	11500	2.0–7.0	6.84 ± 0.21
420	41.0	29.0	3500	1.7–8.6	6.78 ± 0.21
420	44.0	10.0	2000	1.1–8.9	6.54 ± 0.16
420	210.0	1.9	11500	0.6–6.8	6.49 ± 0.12
438	32.0	9.9	1500 ^c	0.2–1.1	7.12 ± 0.17
505	32.0	11.9	1500 ^c	0.3–1.7	10.95 ± 0.77
657	30.0	15.3	1500 ^c	0.1–0.9	16.81 ± 1.90
657	30.0	33.0	1500 ^c	0.1–1.4	17.38 ± 3.19
657	32.0	27.9	6500	0.6–5.0	16.85 ± 0.72
657	32.0	14.3	6500	0.4–4.7	14.21 ± 0.34
657	31.0	28.6	1500	0.3–1.7	15.68 ± 0.65
657	31.5	28.6	1500 ^b	0.7–2.9	15.63 ± 0.36

^a H-atoms produced by N_2H_4 photolysis at 248 nm and laser repetition rate is 10 Hz unless otherwise stated. For a given k_1 determination run, either the laser fluence was kept constant or was varied in accordance with $[\text{N}_2\text{H}_4]$ employed to achieve the desired $[\text{H}]_0$.

^b Laser repetition rate is 2 Hz.

^c H-atoms produced by 193-nm photolysis of N_2H_4 .

^d All errors are 1-sigma.

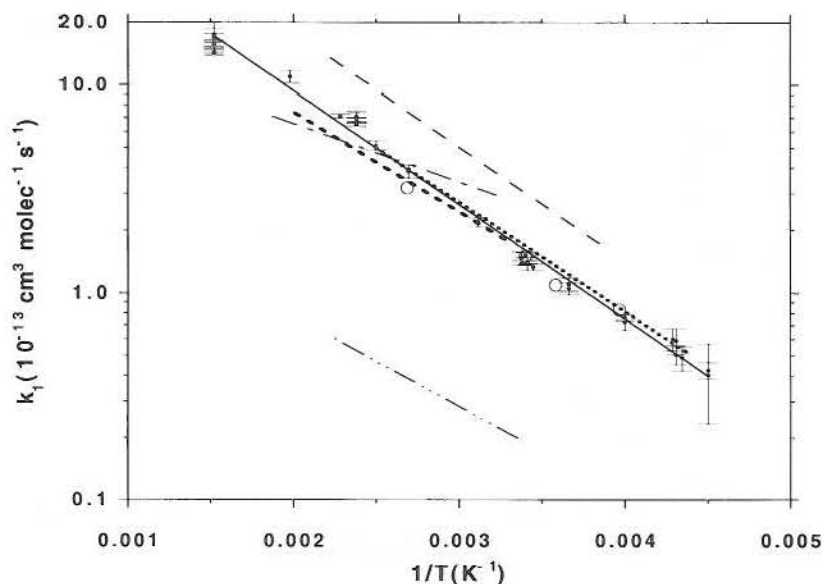


Figure 2. A plot of the absolute second-order rate coefficient, k_1 , for the gas phase reaction $\text{H} + \text{N}_2\text{H}_4 \rightarrow \text{product}$ as a function of $1/T$. Data points are our values obtained in the photolysis work (closed circles with 1-sigma error bars), and in the flow-tube apparatus (open circles). Reference [4] (---), ref. [5] (-.-.-), ref. [6] (- - - - -), ref. [7] (- . - . - . -), and ref. [8] (.....).

Quantum Yield Measurements

Extrapolation of the data in Figure 1 to time zero gives a measure for the primary yield of H-atoms in the photolysis. In the back-to-back 222 and 248-nm photolysis experiments at constant $[\text{N}_2\text{H}_4]$, the ratio, $[\text{H}]_{0,222}/[\text{H}]_{0,248}$, of the initial H-atom yields in the two experiments is given by, $[\text{H}]_{0,222}/[\text{H}]_{0,248} = \Phi_{222}/\Phi_{248} \times \sigma_{222}/\sigma_{248} \times N_{222}/N_{248} \times E_{222}/E_{248}$. Where Φ_{222} and Φ_{248} are the primary H-atom quantum yields, σ_{222} and σ_{248} the absorption cross sections, N_{222} and N_{248} the number of photons per unit energy, and E_{222} and E_{248} the measured fluences, respectively, at 222 and 248 nm. Figure 3 shows our $[\text{H}]_{0,222}/[\text{H}]_{0,248}$ values determined as the ratio of the laser energy E_{222}/E_{248} is varied. The straight line is a linear least-squares fit to the data points forced through the origin. The slope yields a value for the primary quantum yield, Φ_{222} , at 222 nm and is determined to be (1.06 ± 0.01) at 296 K where the indicated error is 1-sigma precision in the fit of the data points. E_{222} was $0.25 \text{ mJ pulse}^{-1} \text{ cm}^{-2}$ and E_{248} ranged from 0.15 to $1.75 \text{ mJ pulse}^{-1} \text{ cm}^{-2}$. We have taken Φ_{248} to be unity, and $\sigma_{248} = 5.88 \times 10^{-20}$ and $\sigma_{222} = 136.3 \times 10^{-20} \text{ cm}^2 \text{ molec}^{-1}$, respectively, at 248 and 222 nm [1].

To calculate the 193-nm primary H-atom quantum yield in N_2H_4 photolysis a comparison of the initial H-atom resonance fluorescence signal can be made to that observed in HBr at constant photolysis laser fluence. However, first we need to account for the attenuation of the observed initial signal that occurs due to the fact that the presence of the photolyte in the reactor causes the resonance fluorescence to degrade differently in the two experiments. Assuming that this attenuation follows a Beer-Lambert relationship, it can then be shown that $\ln\{f_{0,\text{N}_2\text{H}_4}/[\text{N}_2\text{H}_4]\} =$

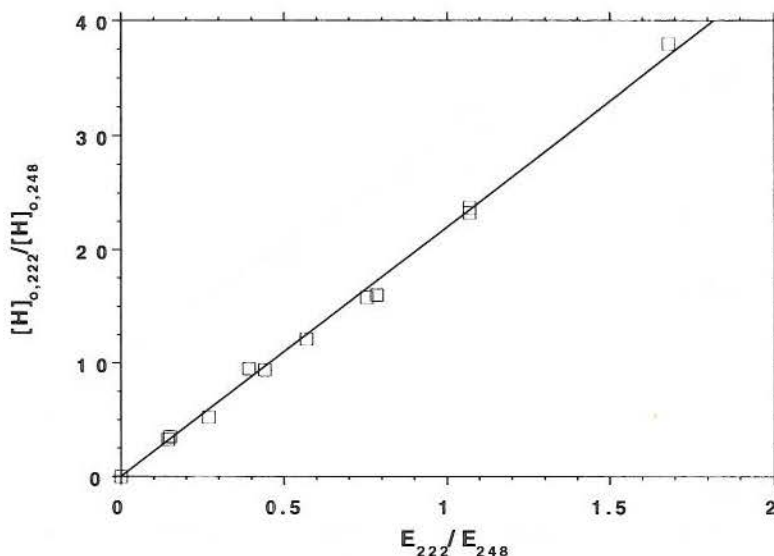


Figure 3. Ratio of initial H-atom yields versus ratio of laser fluences employed in back-to-back 222 and 248-nm photolyses of gaseous N_2H_4 at 296 K. The slope in this plot gives a measure of the 222-nm H-atom primary quantum yield relative to 248-nm photolysis.

$\ln\{I_{N_2H_4}\} - K_{N_2H_4}[N_2H_4]$. Where f_{0,N_2H_4} is the observed initial H-atom signal in hydrazine photolyses, and $K_{N_2H_4}$ is proportional to the product of the effective path length and absorption cross section for the probe radiation in our experiment. $I_{N_2H_4}$ in the above plot is directly proportional to $\Phi_{193} \cdot \sigma_{193}$ for optically thin photolysis conditions. Φ_{193} and $\sigma_{193} = 450 \times 10^{-20} \text{ cm}^2 \text{ molec}^{-1}$ [1] are respectively the primary quantum yield for H-atom production and the absorption cross section at 193 nm in hydrazine. By performing a similar plot for HBr photolyses, the ratio, $I_{N_2H_4}/I_{HBr} = \Phi_{193}\sigma_{193}/\Phi_{HBr}\sigma_{HBr}$ can be used to calculate Φ_{193} . In HBr, the values of the 193-nm primary quantum yield for H-atom production $\Phi_{HBr} = 1$ [26,27] and the absorption cross section $\sigma_{HBr} = 170.3 \times 10^{-20} \text{ cm}^2 \text{ molec}^{-1}$ [28] are used. The typical attenuation of the resonance fluorescence signal in these experiments is shown in Figure 4. We calculate a value of $\Phi_{193} = (1.01 \pm 0.12)$ for the primary quantum yield of H-atom production in 193-nm photolysis of N_2H_4 at 296 K and for $0.35 \text{ mJ pulse}^{-1} \text{ cm}^{-2}$ of laser fluence. The indicated error is 1-sigma, precision plus systematic.

Discussion

H-atom Primary Quantum Yields

To our knowledge, we are the first to report the measurement of the primary quantum yields for H-atom production in 222 and 193-nm photodissociation of hydrazine vapor at 296 K. Since we make a relative determination of the H-atom yield in our work, the accuracy of Φ_{222} and Φ_{193} is determined by how well the ultra-violet absorption cross sections for N_2H_4 and the reference compounds are known. We have recently reported new measurements for the absolute absorption cross

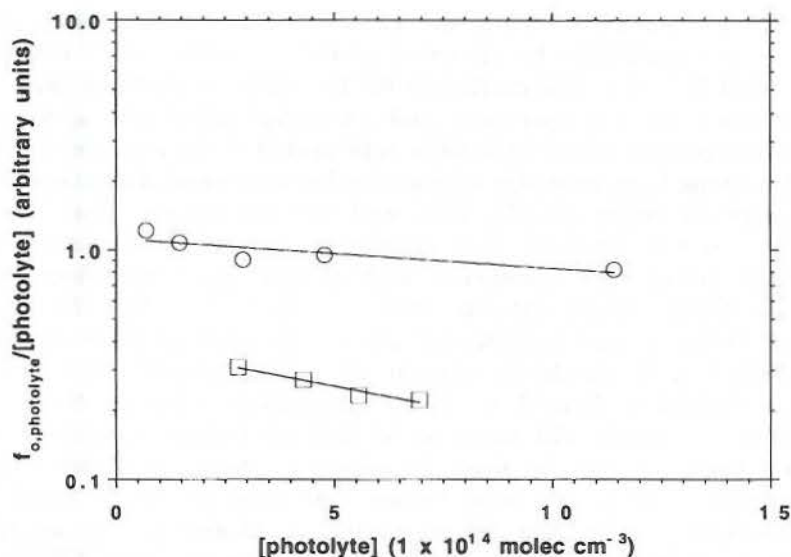


Figure 4. Plots showing the attenuation of the observed initial H-atom fluorescence signals in N₂H₄ (open circles) and HBr (open squares) photolysis at 296 K. The intercepts in these plots are used to calculate the H-atom primary quantum yield in 193-nm photolysis of gaseous N₂H₄ relative to HBr photolysis.

sections for N₂H₄ [1], HBr [28], and CH₃SH [10] that have an overall uncertainty of the order of ca. $\pm 6\%$. However, the relative uncertainty in $\sigma_{222}/\sigma_{248}$ required to calculate Φ_{222} in Figure 3 is expected to be much less $\pm 1\%$ as discussed previously [1]. Assuming Φ_{248} to be unity, we calculate Φ_{222} to be (1.06 ± 0.16) where the error is 1-sigma precision plus systematic. Earlier we had measured Φ_{248} to be (0.85 ± 0.15) based on CH₃SH absorption cross section of $30.0 \times 10^{-20} \text{ cm}^2 \text{ molec}^{-1}$ at 248 nm [29]. When we use our new CH₃SH value of $35.1 \times 10^{-20} \text{ cm}^2 \text{ molec}^{-1}$ [10], Φ_{248} is recalculated to be (0.99 ± 0.17) in better agreement with the expected unit dissociation of N₂H₄ [1]. The value of $\Phi_{193} = (1.01 \pm 0.12)$ we measure here (the error is 1-sigma precision plus systematic) is based on our HBr absorption cross section of $\sigma_{\text{HBr}} = 170.2 \times 10^{-20} \text{ cm}^2 \text{ molec}^{-1}$ which is in good agreement with the currently accepted and recommended value at 193 nm [30–32]. It can be shown that H₂O photolysis at 193 nm ($\sigma = 1.2 \times 10^{-21} \text{ cm}^2 \text{ molec}^{-1}$ [33]) will not interfere with our Φ_{193} measurements for the final hydrazine/water distillate used in our work. To minimize possible H-atom signal from photolysis of photofragments produced in previous laser pulses, we have used low laser repetition rates and sufficient linear flow rates of the gas in the reactor so that the mixture is either completely replaced between the photolytic pulses or is photolyzed only a few times before it is swept away from the reaction zone. Also when measuring Φ_{222} , the relative fluence of the 222 and 248-nm beams, E_{222}/E_{248} , was determined using a calibrated disc calorimeter. We make no corrections to this value for the minute differences in the relative transmission and reflection losses for the two beams passing through the S1-UV optical windows of our reactor. N₂H₄ and HBr are known to be 'sticky' and/or decompose at Pyrex, quartz or stainless steel surfaces [1,34]. Therefore sufficient conditioning of the apparatus was performed so that the losses in photolyte

concentration was negligible during the H-atom yield measurement runs. This is confirmed in our experiments by the value of $(6.52 \pm 0.27) \times 10^{-12} \text{ cm}^3 \text{ molec}^{-1} \text{ s}^{-1}$ we obtain at 296 K for the rate coefficient for $\text{H} + \text{HBr} \rightarrow \text{products}$ [34].

The continuous room temperature and jet-cooled ultraviolet spectra of N_2H_4 and its methylated analogues have been interpreted to be associated with optical excitations involving large geometry changes and/or with rapid dissociation [13,35,36]. Our unit quantum yields at 248, 222, and 193 nm suggest that the first two excited singlet states involved here dissociate to give H-atoms as the major product. These results are consistent with earlier H_2 end-product analysis in hydrazine photolysis which extends into the vacuum-uv [11,37]. The H-atom yield measurements cannot exclude the direct formation of other minor products such as ground state amidogen radical or the previously observed emission from excited amidogen formed in direct photodissociation of N_2H_4 . Quantum yields for these channels will have to be defined before a detailed balance of the observed products can be used to precisely place an upper limit on the relative importance of N—H bond fission compared to N—N bond fission in hydrazine photolysis. Also, the determination of photofragment angular distributions and translational energy measurements using time-of-flight methods would be very useful in obtaining details on the dynamics of N_2H_4 photodissociation.

H + N₂H₄ Absolute Rate Coefficients

We have carried out k_1 rate coefficient measurements for the $\text{H} + \text{N}_2\text{H}_4$ reaction which cover the most extended temperature range in a single photolysis apparatus that utilizes the direct monitoring of $[\text{H}]$ decay profile in a known excess of $[\text{N}_2\text{H}_4]$. In the range 222–657 K, we fit our data to the Arrhenius expression, $k_1 = (11.7 \pm 0.7) \times 10^{-12} \exp[-(2500 \pm 40)/RT] \text{ cm}^3 \text{ molec}^{-1} \text{ s}^{-1}$ ($R(\text{cal mol}^{-1} \text{ K}^{-1})$ is the Gas constant, and $T(\text{K})$ the absolute temperature). The room temperature rate coefficient did not show any pressure dependence in He in the range 24.5–603 torr. Interference on the rate coefficient measurements from possible secondary reactions that consume (or produce) H-atoms was minimized by using large $[\text{N}_2\text{H}_4]/[\text{H}]_0$ ratios. The variation in this ratio (achieved by changing the laser fluence), or the residence time of the $\text{N}_2\text{H}_4/\text{He}$ mixture in the reactor, or the photolysis wavelength used, did not significantly affect the rate coefficient measurements as shown in Table I. Therefore, secondary reactions of H-atoms with N_2H_3 (principle product in N_2H_4 photolysis and $\text{H} + \text{N}_2\text{H}_4$ reaction) or NH_2 (minor product of N_2H_4 photolysis) are not important in our experiments.

Possible decomposition of N_2H_4 in our reactor at high temperatures was briefly investigated by comparing the hydrazine concentration entering the heated cell to that measured at the exit. In the range 657–886 K, a decay coefficient of $(320 \pm 80) \exp[-(4700 \pm 150)/T] \text{ s}^{-1}$ was determined for N_2H_4 in ca. 30 torr He in our quartz cell. The activation energy of ca. 9.3 kcal mol⁻¹ measured here is very indicative of a heterogeneous decomposition process. Homogeneous decomposition of N_2H_4 is expected to be a minor process under our experimental conditions [38]. The decomposition products at the cell walls are expected to be N_2 , H_2 , and NH_3 [39,40]. Appearance of NH_3 in the reaction zone will have a negligible effect on the $[\text{H}]$ decay because of the slow $\text{H} + \text{NH}_3$ reaction rate [41]. In this work we only report $[\text{H}]$ decay measurements below 657 K since hydrazine loss in our cell

is negligible below this temperature. For instance at 657 K we estimate that less than 4% of the hydrazine decomposes heterogeneously in our cell before the heated gas mixture enters the reaction zone. In principle we can measure k_1 above 657 K by making appropriate loss corrections to the photometrically determined $[\text{N}_2\text{H}_4]$. However, this inherently introduces relatively large uncertainties in the k_1 values. For example, the measured value of $k_1(761 \text{ K}) = (21.3 \pm 4.9) \times 10^{-13} \text{ cm}^3 \text{ molec}^{-1} \text{ s}^{-1}$ we determine in this apparatus (after ca. 20% correction) is in good agreement with the value of $22.3 \times 10^{-13} \text{ cm}^3 \text{ molec}^{-1} \text{ s}^{-1}$ we predict from the above Arrhenius expression.

The $\text{H} + \text{N}_2\text{H}_4$ reaction was also studied in a discharge flow-tube apparatus [9]. H-atoms were produced in a side-arm reactor by discharging a 1% H_2/He mixture in a microwave cavity. The discharged products were carried in a 25-mm-id thermostated flow-tube by He at a linear gas flow velocity, v , of 350 cm s^{-1} , and a pressure of 9.5 torr. A known excess of hydrazine was introduced via an axially movable injector. The loss of $[\text{H}]$ in the flow-tube was monitored as a function of the distance, z , between the injector tip, where the two reactants first come in contact, and the fixed detector position situated downstream. A microwave lamp similar to the one described earlier was used to excite the H-atoms in the detection cell. The resultant resonance fluorescence ensuing from the probed volume was viewed at right-angles through a vacuum-monochromator (with a band pass of 1.5 nm, FWHM, and centered at 121.6 nm) and detected by a suitable photomultiplier tube using photon counting methods. The measured pseudo-first-order $[\text{H}]$ decay constants, $k' = -v d(\ln[\text{H}])/dz$, were corrected for the injector wall loss term and the axial radical diffusion term [42]. As before, the absolute second-order rate coefficients were calculated from plots of k' vs. $[\text{N}_2\text{H}_4]$ employed in the flow-tube. The values of $k_1 = (0.83 \pm 0.09) \times 10^{-13}$, $(1.09 \pm 0.12) \times 10^{-13}$, $(1.50 \pm 0.18) \times 10^{-13}$, and $(3.20 \pm 0.48) \times 10^{-13} \text{ cm}^3 \text{ molec}^{-1} \text{ s}^{-1}$ were obtained, respectively, at 252, 279, 294, and 372 K. These data points are in excellent agreement with the photolysis data of Table I, and are shown (without the error bars for clarity) in Figure 2. The fact that we obtain similar k_1 values in two different apparatuses suggest that there are no significant systematic errors in N_2H_4 concentration calculations in our work.

The Arrhenius expression, $(9.87 \pm 1.17) \times 10^{-12} \exp[-(2380 \pm 100)/RT] \text{ cm}^3 \text{ molec}^{-1} \text{ s}^{-1}$, reported by Stief and Payne [8] in the range 228–400 K is in very good agreement with the present study. Their experimental approach was very similar to ours. They produced H-atoms in an excess of N_2H_4 by its flash photolysis (in the wavelength range 144–250 nm) and directly monitored $[\text{H}]$ decay temporal profiles by resonance fluorescence detection of $\text{H}(^2\text{S})$. They measured absolute hydrazine concentrations in the reactor by vacuum-uv photometry. Both this work and that of Stief and Payne is free from interference from secondary reactions of H since very high $[\text{N}_2\text{H}_4]/[\text{H}]_0$ ratios were used. Francis and Jones [7] carried out similar discharge flow-tube experiments as we have, where they monitored pseudo-first-order $[\text{H}]$ decay by esr in an excess of monometrically determined hydrazine concentration (typically the $[\text{N}_2\text{H}_4]/[\text{H}]_0$ ratio was ca. 20). They report the Arrhenius temperature dependence to be $(2.5 \pm 0.5) \times 10^{-12} \exp[-(1300 \pm 200)/RT] \text{ cm}^3 \text{ molec}^{-1} \text{ s}^{-1}$ in the range 311–536 K. Their activation energy, E_a , is ca. 1/2 the value which we report to be $2.5 \text{ kcal mol}^{-1}$, and their room temperature rate coefficient ca. 2 times larger than what we measure. Since secondary reactions of H atoms in their flow-tube should be negligible, it is not clear why both the absolute rate coefficient value and its temperature dependence should differ so much from our flow-tube study or

that of Chobanyan and co-workers' value of $k_1 = (6.8 \pm 1.0) \times 10^{-12} \exp[-(2200 \pm 220)/RT] \text{ cm}^3 \text{ molec}^{-1} \text{ s}^{-1}$ (in the range 305–505 K) [6]. The latter authors also employed esr detection of [H] decay in excess $[\text{N}_2\text{H}_4]$. It is possible that Francis and Jones had systematic $[\text{N}_2\text{H}_4]$ calibration and/or decomposition problems with increasing temperature in their apparatus. Also their room temperature data show a variation in the k_1 value by a factor of almost 2! Gehring et al. [4] used mass spectrometry in their flow-tube work. In excess [H] conditions they monitored $[\text{N}_2\text{H}_4]$ profiles and reported $k_1(303 \text{ K}) = 2.82 \times 10^{-13}$, and in excess $[\text{N}_2\text{H}_4]$ conditions they determined $k_1(300 \text{ K})$ to be $3.16 \times 10^{-13} \text{ cm}^3 \text{ molec}^{-1} \text{ s}^{-1}$ from [H] determinations. Although this shows a self consistency in the rate evaluation procedure, with $k_1 = (21.6 \pm 5.0) \times 10^{-12} \exp[-(2500 \pm 200)/RT] \text{ cm}^3 \text{ molec}^{-1} \text{ s}^{-1}$, in the range 260–450 K, their preexponential factor, A , is ca. 2 times larger but the activation energy is similar to that obtained in the photolysis studies. It is possible that errors in the absolute reagent calibration in their work would result in an erroneous value for the preexponential term. (However, earlier this group had reported $k_1 = 2.82 \times 10^{-13} \text{ cm}^3 \text{ molec}^{-1} \text{ s}^{-1}$ to be independent of temperature in the range 251–315 K [43]).

Schiavello and Volpi [5] studied the reaction in a stirred-flow reactor in the temperature range 298–423 K at ca. 2 torr. Their reported activation energy is similar in value to ours but the preexponential factor is ca. 20 times smaller ($k_1 = 5.8 \times 10^{-13} \exp[-2000/RT] \text{ cm}^3 \text{ molec}^{-1} \text{ s}^{-1}$). From the steady-state mass-spectrometric measurements of N_2H_4 and the products NH_3 and N_2 , Schiavello and Volpi showed that the ratio of $\text{NH}_3:\text{N}_2$ formed was 2, and the ratio of $\text{NH}_3:\text{N}_2\text{H}_4$ consumed was 1 throughout the range of $[\text{N}_2\text{H}_4]_0/[\text{H}]_0 < \text{ca. } 2.3$ employed in their work. When D was reacted with N_2H_4 , they saw no NH_2D , and at low in-flowing N_2H_4 concentrations mainly HD was produced, while in excess $[\text{N}_2\text{H}_4]$ conditions H_2 and $\text{N}_2\text{H}_3\text{D}$ were also observed as minor products. These observations suggest a mechanism in which the atomic hydrogen abstracts an H-atom from the N—H bond in hydrazine, and also the occurrence of the isotope exchange reaction, $\text{D} + \text{N}_2\text{H}_4 \rightarrow \text{H} + \text{N}_2\text{H}_3\text{D}$, where the H goes on further to react with hydrazine in an abstraction reaction to give H_2 . Ghosh and Bair [44] studied the greenish-yellow luminescence at ca. 590 nm that was produced in their flow reactor when a large excess (>500–5000) of H-atoms (formed in a discharge) were reacted with N_2H_4 . They identified $\text{NH}_2(\text{A})$ to be the emitting species and found the emission to be directly proportional to $[\text{N}_2\text{H}_4]$. The yield of this emission per N_2H_4 molecule consumed was measured to be very small, ca. 0.000131 to ca. 0.000154 in the range 293–349 K suggesting that the process $\text{H} + \text{N}_2\text{H}_4 \rightarrow \text{NH}_2(\tilde{\text{A}}^2\text{A}_1) + \text{NH}_3$ must be a minor reaction channel in the overall consumption mechanism of hydrazine in their cell.

Thus the lack of pressure dependence of k_1 in our work, and the very small $\text{NH}_2(\text{A})$ luminescence yields in Ghosh and Bair's work, and the lack of NH_2D formation in the isotopically mixed reaction, $\text{D} + \text{N}_2\text{H}_4$, studied by Schiavello and Volpi suggests that the reaction of atomic hydrogen with hydrazine proceeds by H-abstraction and not via N-attack. Upon combining the individual k_1 determinations of this work with that of Stief and Payne, and of Chobanyan et al., we obtain the Arrhenius expression, $k_1 = (11.0 \pm 1.0) \times 10^{-12} \exp[-(2460 \pm 100)/RT] \text{ cm}^3 \text{ molec}^{-1} \text{ s}^{-1}$, for the temperature dependence of the rate coefficient, k_1 , for the reaction, $\text{H} + \text{N}_2\text{H}_4 \rightarrow \text{H}_2 + \text{N}_2\text{H}_3$, in the range 222–657 K. The indicated error, σ_{Ea} , is 1-sigma in the fit of the data points, and $\sigma_{\text{A}} = A\sigma_{\ln A}$.

Acknowledgment

This work was supported by the Air Force Office for Scientific Research and was carried out under contract # F04611-93-C-0005 at Phillips Laboratory, Edwards AFB, California.

Bibliography

- [1] G. L. Vaghjiani, *J. Chem. Phys.*, **98**, 2123 (1993).
- [2] D. F. Strobel, *J. Atmos. Sci.*, **30**, 1205 (1973); and *Rev. Geophys. Space Phys.*, **13**, 372 (1975).
- [3] E. W. Schmidt, *Hydrazine and Its Derivatives: Preparation, Properties, Applications*, Wiley, New York, 1984.
- [4] M. Gehring, K. Hoyer mann, H. Gg. Wagner, and J. Wolfrum, *Ber. Bunsenges. Phys. Chem.*, **75**, 1287 (1971).
- [5] M. Schiavello and G. G. Volpi, *J. Chem. Phys.*, **37**, 1510 (1962).
- [6] S. A. Chobanyan, T. G. Mkryan, and E. N. Sarkisyan, *Kinet. Catal.*, **26**, 857 (1985).
- [7] P. D. Francis and A. R. Jones, *J. Chem. Phys.*, **54**, 5085 (1971).
- [8] L. J. Stief and W. A. Payne, *J. Chem. Phys.*, **64**, 4892 (1976).
- [9] G. L. Vaghjiani, *J. Phys. Chem.*, to be submitted.
- [10] G. L. Vaghjiani, *J. Chem. Phys.*, **99**, 5936 (1993) and references therein.
- [11] U. Schurath and R. N. Schindler, *J. Phys. Chem.*, **74**, 3188 (1970).
- [12] B. Ruscic and J. Berkowitz, *J. Chem.*, **95**, 4378 (1991).
- [13] V. Staemmler, *Acta Phys. Pol. A*, **74**, 331 (1988) and references therein.
- [14] H. Biehl and F. Stuhl, *J. Photochem. Photobiol. A: Chem.*, **59**, 135 (1991).
- [15] A. Hopkirk, J. A. Salthouse, R. W. P. White, J. C. Whitehead, and F. Winterbottom, *Chem. Phys. Lett.*, **188**, 399 (1992).
- [16] V. I. Lang, *J. Quant. Spectrosc. Radiat. Transfer*, **52**, 45 (1994).
- [17] P. Lindberg, D. Raybone, J. A. Salthouse, T. M. Watkinson, and J. C. Whitehead, *Mol. Phys.*, **62**, 1297 (1987).
- [18] I. P. Vinogradov and V. V. Firsov, *Opt. Spectrosc. USSR*, **53**, 26 (1982).
- [19] G. Herzberg, *Molecular Spectra and Molecular Structure III Electronic Spectra and Electronic Structure of Polyatomic Molecules*, Krieger, 1991; and M. W. Chase, Jr., C. A. Davies, J. R. Downey, Jr., D. J. Frurip, R. A. McDonald, and A. N. Syverud, *J. Phys. Chem. Ref. Data*, **14**, Suppl. 1 (1985).
- [20] W. G. Hawkins and P. L. Houston, *J. Phys. Chem.*, **86**, 704 (1982).
- [21] D. A. Ramsay, *J. Phys. Chem.*, **57**, 415 (1953).
- [22] D. Husain and R. G. W. Norrish, *Proc. R. Soc. London, Ser. A*, **273**, 145 (1963).
- [23] M. Arvis, C. Devillers, and M. Gillois, *J. Phys. Chem.*, **78**, 1356 (1974).
- [24] G. L. Vaghjiani and A. R. Ravishankara, *J. Chem. Phys.*, **92**, 996 (1990).
- [25] J. Park, N. Shafer, and R. Bersohn, *J. Chem. Phys.*, **91**, 7861 (1989).
- [26] R. M. Martin and J. E. Willard, *J. Chem. Phys.*, **40**, 2999 (1964).
- [27] G. Radhakrishnan, S. Buelow, and C. Wittig, *J. Chem. Phys.*, **84**, 727 (1986).
- [28] G. L. Vaghjiani, *UV Mechanisms: Laboratory Photochemical Decomposition Studies of Hydrazine*, Tech. Rep. UDR-TR-93-67, University of Dayton Research Institute, Dayton, Ohio, 1993.
- [29] J. G. Calvert and J. N. Pitts, Jr., *Photochemistry*, Wiley, New York, 1966.
- [30] B. J. Huebert and R. M. Martin, *J. Phys. Chem.*, **72**, 3046 (1968).
- [31] C. F. Goodeve and A. W. C. Taylor, *Proc. Roy. Soc.*, **A152**, 221 (1935).
- [32] G. L. Vaghjiani, A. A. Turnipseed, R. F. Warren, and A. R. Ravishankara, *J. Chem. Phys.*, **96**, 5878 (1992).
- [33] M. Nicolet, *Etude des Reactions Chimiques de l'Ozone dans la Stratosphere*, Institut Royal Meteorologique de Belgique, 1990.
- [34] R. K. Talukdar, R. F. Warren, G. L. Vaghjiani, and A. R. Ravishankara, *Int. J. Chem. Kinet.*, **24**, 973 (1992) and references therein.
- [35] J. A. Syage, R. B. Cohen, and J. Steadman, *J. Chem. Phys.*, **97**, 6072 (1992).
- [36] E. M. Evleth, *Chem. Phys. Lett.*, **38**, 516 (1976).
- [37] L. J. Stief, V. J. DeCarlo, and R. J. Mataloni, *J. Chem. Phys.*, **15**, 592 (1967).

- [38] E. Meyer, H. A. Olschewski, J. Troe, and H. Gg. Wagner, *Symp. (Int.) Combust. Proc.*, **12**, 345 (1969).
- [39] C. H. Bamford, *Trans. Faraday Soc.*, **35**, 1239 (1939).
- [40] T. J. Hanratty, J. N. Pattison, and J. W. Clegg, *Ind. Chem. Eng. Anal.*, **43**, 1113 (1950).
- [41] T. Ko, P. Marshall, and A. Fontijn, *J. Phys. Chem.*, **94**, 1401 (1990).
- [42] C. J. Howard, *J. Phys. Chem.*, **83**, 3 (1979).
- [43] M. Gehring, K. Hoyer mann, H. Gg. Wagner, and J. Wolfrum, *Ber. Bunsenges. Phys. Chem.*, **73**, 956 (1969).
- [44] P. K. Ghosh and E. J. Bair, *J. Chem. Phys.*, **45**, 4738 (1966).

Received November 28, 1994

Accepted January 25, 1995